NASA Contractor Report 187457
ICASE Report No. 90–73

ICASE

SPURIOUS FREQUENCIES AS A RESULT OF NUMERICAL BOUNDARY TREATMENTS

Saul Abarbanel
David Gottlieb

Contract No. NAS1–18605
October 1990

Institute for Computer Applications in Science and Engineering
NASA Langley Research Center
Hampton, Virginia 23665–5225

Operated by the Universities Space Research Association

National Aeronautics and
Space Administration

Langley Research Center
Hampton, Virginia 23665-5225

SPURIOUS FREQUENCIES AS A RESULT OF NUMERICAL BOUNDARY TREATMENTS

Saul Abarbanel[1]
Department of Mathematical Sciences
Division of Applied Mathematics
Tel-Aviv University
Tel-Aviv, ISRAEL

and

David Gottlieb[1]
Division of Applied Mathematics
Brown University
Providence, RI 02192

ABSTRACT

The stability theory for finite difference Initial Boundary-Value approximations to systems of hyperbolic partial differential equations states that the exclusion of eigenvalues and generalized eigenvalues is a sufficient condition for stability. The theory, however, does not discuss the nature of numerical approximations in the presence of such eigenvalues.

In fact, as was shown previously [1], for the problem of vortex shedding by a 2-D cylinder in subsonic flow, stating boundary conditions in terms of the primitive (non-characteristic) variables may lead to such eigenvalues, causing perturbations that decay slowly in space and remain periodic time. Characteristic formulation of the boundary conditions avoided this problem.

In this paper, we report on a more systematic study of the behavior of the (linearized) one-dimensional gas dynamic equations under various sets of oscillation-inducing "legal" boundary conditions.

[1]This research was supported by the National Aeronautics and Space Administration under NASA Contract No. NAS1-18605 while the authors were in residence at the Institute for Computer Applications in Science and Engineering (ICASE), NASA Langley Research Center, Hampton, VA 23665. The second author was also supported by the Air Force Office of Scientific Research Grant No. AFOSR-90-0093, by DARPA-URI Contract N00014-86-k0754, and by NSF Grant DMS-88-10150.

1. Introduction

The increase in computers' speed and memory allows researchers to investigate fluid dynamical problems with greater attention to delicate features of the flows. For example, only in the last five years have investigators [1,6] computed the vortex shedding phenomenon behind a two-dimensional cylinder at low Mach numbers and moderate Reynolds numbers. Unfortunately, with this improved ability due to increased computer power to compute complex phenomena comes the necessity to deal with unforeseen numerical surprises which might be mistaken for real or physical effects. For example, in the case of the 2-D cylindrical Von-Karman vortex street computation – the main features of the flow, such as the shedding frequency are predicted accurately. However, a concomitant computational result appearing in the output data base is a spurious secondary frequency which was mistakingly attributed to the start of transition. In previous work, [1], we have shown that the spurious secondary frequency resulted from applying the far-field inflow boundary condition to the primitive variables. It was also shown there that the same boundary treatment, applied, however, to the characteristic variables, eliminated this phenomenon. In this paper, we characterize, by an analytic description, the boundary conditions (both inflow and outflow) under which the numerical solution of the Euler equations will exhibit temporal oscillations which are foreign to the exact solution of the p.d.e.'s. The starting point of our study is the modal analysis developed by G-K-S [2], and Osher [3]. This theory states that for finite differences approximations to Initial Boundary Value problems of hyperbolic systems stability is assured by the exclusion of eigenvalues and generalized eigenvalues. The theory, however, does not discuss the nature of the numerical approximations in the presence of such eigenvalues.

The model that we study is that of the 1-D compressible Euler equations linearized about free stream conditions. The numerical schemes that we analyze are second order in space and time represented by the Lax-Wendroff scheme. In our 1-D case it is equivalent to all other second order algorithms such as the MacCormack scheme [4].

In Section 2, we briefly review the underlying theoretical considerations both for the p.d.e. and the f.d.e. formulation.

In Section 3, we discuss the case of inflow b.c.'s expressed with primitive variables. We show that even though the numerical solution is technically stable and therefore, by the Lax equivalence theorem, convergent, for finite meshes and time it shows spurious oscillations that decay only slowly with mesh refinement. In Section 4, we repeat this demonstration for the case of primitive-variable description of the out-flow boundary conditions. In Section 5, we apply a primitive-variable formulation of the boundary conditions both at the inflow and outflow boundaries. This allows a nonlinear interaction between the modes created at both boundaries. At this point, the reader should be reminded that the same treatment of the boundary conditions, applied to the characteristic variables eliminates any spurious frequencies. This is a corollary of our analytical formulation and is borne out in our numerical experiments.

All sections contain numerical examples pertinent to the initial boundary value problem considered therein.

2. Analytical Preliminaries

We start with the one-dimensional Euler equations of gas dynamics in conservation form:

$$\frac{\partial U}{\partial t} + \frac{\partial F(U)}{\partial x} = 0 \tag{2.1}$$

where

$$U = \begin{bmatrix} \rho \\ m \\ E \end{bmatrix}, \tag{2.2}$$

$$F = \begin{bmatrix} m \\ \frac{m^2}{\rho} + p \\ u(E+p) \end{bmatrix}. \tag{2.3}$$

Here u, ρ, p and E are, respectively, the velocity, density, pressure, and total energy per unit volume. $m = \rho u$ is the mass flux. In the case of an ideal gas the equation of state is

$$p = (\gamma - 1)\left[E - \frac{1}{2}\left(\frac{m^2}{\rho}\right)\right] \tag{2.4}$$

where $\gamma = 7/5$ for diatomic gases such as air. Equation (2.1) can be rewritten in non-conservation form as

$$\frac{\partial U}{\partial t} + A(U)\frac{\partial U}{\partial x} = 0 \tag{2.5}$$

where $A = \partial F/\partial U$ is the Jacobian of the flux vector F with respect to the solution vector U. Linearizing about steady free stream conditions, $U_\infty^T = (\rho_\infty, \rho_\infty u_\infty, E_\infty)$, Equation (2.5) becomes:

$$\frac{\partial}{\partial t}(\delta U) + A(U_\infty)\frac{\partial}{\partial x}(\delta U) = 0, \tag{2.6}$$

where $\delta U = U - U_\infty$ is the perturbation vector. The matrix $A(U_\infty) = \left[\frac{\partial F(U)}{\partial U}\right]_{U=U_\infty}$ has three eigenvalues, $a_1 = u_\infty - c_\infty, a_2 = u_\infty + c_\infty$ and $a_3 = u_\infty$. The free stream sound speed, c_∞, is given by $c_\infty = (\gamma p_\infty/\rho_\infty)^{\frac{1}{2}}$. The corresponding eigenvectors in terms of the conserved-variable perturbations are given by

$$R_1 = -(\delta m - u_\infty \delta\rho) + \frac{\gamma - 1}{c_\infty}\left[\frac{1}{2}u_\infty^2 \delta\rho - u_\infty \delta m + \delta E\right], \tag{2.7}$$

$$R_2 = (\delta m - u_\infty \delta\rho) + \frac{\gamma - 1}{c_\infty}\left[\frac{1}{2}u_\infty^2 \delta\rho - u_\infty \delta m + \delta E\right], \tag{2.8}$$

and

$$R_3 = c_\infty \delta\rho - \frac{\gamma - 1}{c_\infty}\left[\frac{1}{2}u_\infty^2 \delta\rho - u_\infty \delta m + \delta E\right]. \tag{2.9}$$

Furthermore, using a linearized version of the equation of state, i.e.,

$$\delta p = (\gamma - 1)\left[\frac{1}{2}u_\infty^2 \delta\rho - u_\infty \delta m + \delta E\right], \tag{2.10}$$

equations (2.7) - (2.9) may also be written in terms of the primitive-variable perturbations, $(\delta p, \delta u, \delta \rho)$:

$$R_1 = -\rho_\infty \delta u + \frac{1}{c_\infty}\delta p, \tag{2.11}$$

$$R_2 = \rho_\infty \delta u + \frac{1}{c_\infty}\delta p, \tag{2.12}$$

and

$$R_3 = c_\infty \delta \rho - \frac{1}{c_\infty}\delta p. \tag{2.13}$$

Any perturbation imposed on the free stream solution will evolve as a combination of these eigenvectors.

In terms of the characteristic variables $R_s (s = 1, 2, 3)$ defined in (2.7 - 2.9) and/or (2.11 - 2.13), Equation (2.6) may be written as:

$$\frac{\partial R_1}{\partial t} + (u_\infty - c_\infty)\frac{\partial R_1}{\partial x} = 0 \tag{2.14}$$

$$\frac{\partial R_2}{\partial t} + (u_\infty + c_\infty)\frac{\partial R_2}{\partial x} = 0 \tag{2.15}$$

$$\frac{\partial R_3}{\partial t} + u_\infty \frac{\partial R_3}{\partial x} = 0 \tag{2.16}$$

or

$$\frac{\partial R_s}{\partial t} + a_s \frac{\partial R_s}{\partial x} = 0, \quad s = 1, 2, 3. \tag{2.17}$$

In a finite domain, say $0 < x < 1$, for the subsonic case $u_\infty < c_\infty$, the system (2.7) is well posed with the following initial and boundary conditions:

$$R_s(x, 0) = f_s(x) \quad s = 1, 2, 3 \tag{2.18}$$

$$R_2(0, t) - \alpha_0 R_1(0, t) = g_1(t) \tag{2.19}$$

$$R_3(0, t) - \beta_0 R_1(0, t) = g_2(t) \tag{2.20}$$

$$R_1(1, t) + \sigma_1 R_2(1, t) + \varepsilon_1 R_3(1, t) = g_3(t) \tag{2.21}$$

where $\alpha_0, \beta_0, \sigma_1$ and ε_1 are arbitrary real constants and $f_s(x), g_s(t) \quad (s = 1, 2, 3)$ are square integrable in their respective domains.

We get numerical approximations of second order spatial and temporal accuracy by using the Lax-Wendroff scheme,

$$w_j^{s,n+1} = w_j^{s,n} - \frac{a_s \Delta t}{2\Delta x}(w_{j+1}^{s,n} - w_{j-1}^{s,n}) + \frac{a_s^2 (\Delta t)^2}{2(\Delta x)^2}(w_{j+1}^{s,n} - 2w_j^{s,n} + w_{j-1}^{s,n}), \quad j > 0 \quad s = 1, 2, 3 \tag{2.22}$$

where $w_j^{s,n} = w^s(j\Delta x, n\Delta t)$ is the finite difference approximation to $R_s(x, t)$.

We note at this junction that although we shall illustrate the detailed development of the spurious frequencies using the Lax-Wendroff scheme, they depend in fact mostly on the form of the finite-difference boundary conditions (yet to be specified) and not on the particular inner algorithm.

To close the system (2.22) we need both the finite difference form of the algebraic boundary conditions (2.19 - 2.22) i.e.,

$$w_0^{2,n} - \alpha_0 w_0^{1,n} = g_1(n\Delta t) \tag{2.23}$$

$$w_0^{3,n} - \beta_0 w_0^{1,n} = g_2(n\Delta t) \tag{2.24}$$

$$w_N^{1,n} + \sigma_1 w_N^{2,n} + \varepsilon_1 w_N^{3,n} = g_3(n\Delta t) \tag{2.25}$$

and also three "numerical" boundary conditions, one at $x = 0$ and two at $x = 1 = \Delta x N$. A commonly used method of imposing "numerical" boundary condition is to extrapolate from the interior in the following manner:

$$w_0^{1,n} + \sigma_0 w_0^{2,n} + \varepsilon_0 w_0^{3,n} = w_1^{1,n} + \sigma_0 w_1^{2,n} + \varepsilon_0 w_1^{3,n}, \tag{2.26}$$

and at the outflow boundary, $x = 1 = N\Delta x$,

$$w_N^{2,n} - \alpha_1 w_N^{1,n} = w_{N-1}^{2,n} - \alpha_1 w_{N-1}^{1,n}, \tag{2.27}$$

$$w_N^{3,n} - \beta_1 w_N^{1,n} = w_{N-1}^{3,n} - \beta_1 w_{N-1}^{1,n}. \tag{2.28}$$

The "numerical" boundary conditions (2.26) - (2.28) are zeroth order extrapolations, with $\alpha_1, \beta_1, \sigma_0$ and ε_0 arbitrary real constants.

For stability analysis studies it is sufficient to consider the case of homogeneous boundary conditions, i.e., $g_r(n\Delta t) = 0, r = 1, 2, 3$. We look for solutions of the form

$$w_j^{s,n} = z^n(A_s \kappa_s^j + B_s \mu_s^j), \quad s = 1, 2, 3. \tag{2.29}$$

Substituting this ansatz into (2.22) we find that the κ_s's and μ_s's are the roots of the quadratic equation

$$(\lambda_s^2 - \lambda_s)\chi_s^2 + 2(1 - z - \lambda_s^2)\chi_s + (\lambda_s^2 + \lambda_s) = 0 \tag{2.30}$$

where $\lambda_s = a_s \Delta t / \Delta x$. For $|z| > 1$ one of the roots of (2.30) (say κ_s) is inside the unit circle and the other, μ_s, is outside the unit circle.

Substituting (2.29) into the homogeneous version of (2.23) - (2.28) we get the following system of equations:

$$Q(\kappa_s(z), \mu_s(z)) \begin{pmatrix} A_1 \\ A_2 \\ A_3 \\ B_1 \\ B_2 \\ B_3 \end{pmatrix} = 0 \tag{2.31}$$

where $Q(\kappa_s(z), \mu_s(z)) \triangleq Q(z)$ is given by

$$\begin{bmatrix}
\kappa_1 - 1 & \sigma_0(\kappa_2 - 1) & \varepsilon_0(\kappa_3 - 1) & \mu_1 - 1 & \sigma_0(\mu_2 - 1) & \varepsilon_0(\mu_3 - 1) \\
-\alpha_0 & 1 & 0 & -\alpha_0 & 1 & 0 \\
-\beta_0 & 0 & 1 & -\beta_0 & 0 & 1 \\
\kappa_1^N & \sigma_1\kappa_2^N & \varepsilon_1\kappa_3^N & \mu_1^N & \sigma_1\mu_2^N & \varepsilon_1\mu_3^N \\
-\alpha_1\kappa_1^{N-1}(\kappa_1 - 1) & \kappa_2^{N-1}(\kappa_2 - 1) & 0 & -\alpha_1\mu_1^{N-1}(\mu_1 - 1) & \mu_2^{N-1}(\mu_2 - 1) & 0 \\
-\beta_1\kappa_1^{N-1}(\kappa_1 - 1) & 0 & \kappa_3^{N-1}(\kappa_3 - 1) & -\beta_1\mu_1^{N-1}(\mu_1 - 1) & 0 & \mu_3^{N-1}(\mu_3 - 1)
\end{bmatrix}. \tag{2.32}$$

Note that the dependency on z in (2.32) comes from the fact that $\kappa_j, \mu_j \quad (j = 1, 2, 3)$ are functions of z defined implicitly in (2.30).

It is quite easy to formulate a necessary condition for stability. This is the Riabenkii-Godunov condition [5]:

Lemma 2.1: *The Lax-Wendroff scheme (2.22) with the inflow boundary conditions (2.23), (2.24), and (2.26) and outflow conditions (2.25), (2.27), (2.28) is unstable if there is* $|z_0| > 1$ *such that*

$$\det Q(z_0) = 0. \tag{2.33}$$

In fact, such a z_0 gives a solution of the type

$$w_j^{s,n} = z_0^n(A_s\kappa_s^j + B_s\mu_s^j)$$

that grows with the number of time steps. This is indeed a case of classical instability.

The sufficient condition for stability can also be formulated in terms of the determinant of $Q(z)$; in fact it has been proven:

Lemma (2.2): [GKS] *The LW scheme (2.22) with the b.c.'s (2.23) - (2.28) is stable if for every* $|z_0| \geq 1$,

$$\det Q(z_0) \neq 0 \tag{2.34}$$

It is evident that the case $|z_0| = 1$ with $\det Q(z_0) = 0$ is covered by neither lemma. It is precisely this case, however, that is responsible for the spurious oscillations.

For the sake of convenience, we rewrite (2.31) and (2.32) in the following way:

Define

$$A(\kappa) = \begin{pmatrix} \kappa_1 - 1 & \sigma_0(\kappa_2 - 1) & \varepsilon_0(\kappa_3 - 1) \\ -\alpha_0 & 1 & 0 \\ -\beta_0 & 0 & 1 \end{pmatrix}$$

$$B(\kappa) = \begin{pmatrix} \kappa_1^N & \sigma_1\kappa_2^N & \varepsilon_1\kappa_3^N \\ -\alpha_1\kappa_1^{N-1}(\kappa_1 - 1) & \kappa_2^{N-1}(\kappa_2 - 1) & 0 \\ -\beta_1\kappa_1^{N-1}(\kappa_1 - 1) & 0 & \kappa_3^{N-1}(\kappa_3 - 1) \end{pmatrix} \tag{2.35}$$

$$\vec{a} = \begin{pmatrix} A_1 \\ A_2 \\ A_3 \end{pmatrix} \quad \vec{b} = \begin{pmatrix} B_1 \\ B_2 \\ B_3 \end{pmatrix}.$$

Now (2.31) becomes

$$A(\kappa)\,\vec{a} + A(\mu)\,\vec{b} = 0 \tag{2.36a}$$

$$B(\kappa)\,\vec{a} + B(\mu)\,\vec{b} = 0 \tag{2.36b}$$

and

$$Q(z) = \begin{pmatrix} A(\kappa) & A(\mu) \\ B(\kappa) & B(\mu) \end{pmatrix} \tag{2.37}$$

The determinant condition (2.33) involves the solution of a very complicated nonlinear complex equation. Only little insight can be gained by trying to directly analyze it. One simple case, though, is given by the **fully characteristic** case

$$\alpha_0 = \beta_0 = \sigma_0 = \varepsilon_0 = \alpha_1 = \beta_1 = \sigma_1 = \varepsilon_1 = 0. \tag{2.38}$$

Note that in this case A and B are diagonal

$$A(\kappa) = \begin{pmatrix} \kappa_1 - 1 & 0 & 0 \\ 0 & 1 & 0 \\ 0 & 0 & 1 \end{pmatrix} \quad B(\kappa) = \begin{pmatrix} \kappa_1^N & 0 & 0 \\ 0 & \kappa_2^{N-1}(\kappa_2 - 1) & 0 \\ 0 & 0 & \kappa_3^{N-1}(\kappa_3 - 1) \end{pmatrix} \tag{2.39}$$

and the determinant condition reduces to

$$[(\kappa_1 - 1)\mu_1^N - \kappa_1^N(\mu_1 - 1)][(\mu_2 - 1)\mu_2^{N-1} - \kappa_2^{N-1}(\kappa_2 - 1)][(\mu_3 - 1)\mu_3^{N-1} - \kappa_3^{N-1}(\kappa_3 - 1)] = 0. \tag{2.40}$$

Equation (2.40) indicates that the choice of parameters in (2.38) decouples the system (2.31) and the system is thus reduced to the scalar case. It may be easily shown, using (2.30), that there is no z_0 for which (2.40) has a solution, and therefore no spurious solutions exist in the fully characteristic case.

3. The Inflow Case

In this section, we will investigate the possibility of having a spurious frequency induced by "primitive" boundary conditions (numerical and analytical) at the inflow boundary. By "primitive" boundary conditions, we mean b.c.'s expressed in terms of primitive variables. By a spurious frequency, we mean a solution of the type $z_0 = e^{i\phi}$ to the determinant condition (2.33). Indeed, if the determinant has such a root z_0, then a spurious solution of the form

$$w_j^{s,n} = z^n(A_s\kappa_s^j + B_s\mu_s^j) = e^{in\phi}(A_s\kappa_s^j + B_s\mu_s^j) \tag{3.1}$$

is superimposed on any numerical solution of (2.22) - (2.28).

When the number of grid point increases without limit, $N \longrightarrow \infty$, the influence of the outflow boundary treatment gets decoupled from that of the inflow boundary. This can be seen by observing that the submatrix $B(\kappa)$ defined in (2.35) vanishes because $|\kappa| < 1$. At the same time $B(\mu)$ tends to infinity. Therefore, from (2.36b) we have that $\vec{b} \rightarrow 0$. We have then, from (2.36a)

$$A(\kappa)\,\vec{a} = 0 \tag{3.2}$$

and the determinant condition (2.32) reduces by (2.37) to

$$\det Q(z) = (\kappa_1 - 1) + \sigma_0\alpha_0(\kappa_2 - 1) + \varepsilon_0\beta_0(\kappa_3 - 1) = 0. \tag{3.3}$$

In practice, one cannot achieve $N \rightarrow \infty$. We then inquire how to best decouple the outflow influence from the inflow for the case of fixed N, albeit large. If we set the amplitude of the perturbations due to outflow treatment, $|\ \vec{b}\ |$, equal to zero then from (2.36) we have

$$(A(\kappa) + B(\kappa))\,\vec{a} = 0 \tag{2.36c}$$

as well as $A(\kappa)\,\vec{a} = 0$. Thus the term $B(\kappa)$ in (2.36c) represents the effect of the incomplete decoupling due to the finite N. Since $N \gg 1$, it is clear from the definitions that $B(\kappa)$ represents a small perturbation to $A(\kappa)$, which we would like to minimize. It can be shown that this minimization is achieved for $\varepsilon_1 = \sigma_1 = \alpha_1 = \beta_1 = 0$. Notice that this corresponds to imposing both analytic and numerical outflow boundary conditions on the characteristic variables, $R_s(s = 1, 2, 3)$.

A spurious solution exists if the determinant condition (3.3) has a root of the form $z_0 = e^{i\phi}$. In this case, the homogeneous version of (2.21) - (2.28) with $\sigma_1 = \varepsilon_1 = \alpha_1 = \beta_1 = 0$ admits a solution of the form

$$w_j^{s,n} = A_s e^{in\phi}\kappa_s^j, \quad \phi \neq 0 \tag{3.4}$$

$$|\kappa_s(e^{in\phi})| < 1. \tag{3.5}$$

Several observations can be made at this stage:

(i) No spurious frequency is created if either the analytical inflow boundary conditions (2.23) - (2.24) or the numerical one (2.25) are in characteristic form.

If the analytical boundary conditions are in characteristic form, then $\alpha_0 = \beta_0 = 0$ and the system case is reduced to the scalar case. If the numerical inflow condition (2.26) is in characteristic form, then $\sigma_0 = \varepsilon_0 = 0$ and the system again reduces to the scalar case.

(ii) On the other hand, if the inflow boundary conditions are not given in terms of characteristic variables, then there is a wealth of possible boundary treatments that lead each to different spurious solutions. In fact, for every frequency there exists a set of inflow boundary conditions that induces a spurious solution with that frequency. In particular, given an arbitrary $z_0 = e^{i\phi}; \phi \neq 0$ we get $\kappa_s(z_0)$ from (2.30). We can then view (3.3) as an equation for $\alpha_0\sigma_0$ and $\beta_0\varepsilon_0$. Since these quantities are real, whereas the $\kappa_s(z_0)$ are complex, Equation (3.3) is a system of two equations for $\alpha_0\sigma_0$ and $\beta_0\varepsilon_0$, yielding a unique solution. The explicit form of the spurious solution (3.4) reveals the nature of such a solution. We summarize the results in the results in the following lemma:

Lemma (3.1): *The spurious solution (3.4) converges to zero for every fixed $x = j\Delta x$ and $t = n\Delta t$ as $\Delta x \to 0, \Delta t \to 0$.*

Proof: Since $\Delta x \to 0$ and x is fixed, then $j \to \infty$. Note that $|\kappa_s| < 1$, and therefore $\lim_{j\to 0} \kappa_s^j = 0$.

Notice that even though Lemma (3.1) indicates convergence of the total scheme, still on a fixed finite grid, the spurious solution

$$w_j^{s,n} = A_s e^{in\phi}\kappa_s^j$$

may be confused with a real time periodic solution. In particular, if one of the $\kappa_s(e^{i\phi})$ is close to unity in magnitude, then the time periodic solution may show up in a large part of the spatial domain. Of course, if all the κ's are small in magnitude, the time periodic spurious solution will be confined to a very narrow boundary layer at the inflow boundary.

To illustrate the above analysis, we chose to solve numerically equations (2.14) - (2.16) with $u_\infty = 1$ and $M_\infty = .4$. Thus, $a_1 = -1.5; a_2 = 3.5; a_3 = 1; c_\infty = 2.5$. For the initial conditions (2.18), we chose

$$R_1(x,0) = e^{-x} \quad R_2(x,0) = e^{x} \quad R_3(x,0) = e^{2x}. \tag{3.7}$$

For the analytical boundary conditions (2.19) - (2.21), we chose

$$\alpha_0 = .582155; \quad \beta_0 = -.6115; \quad \sigma_1 = 0; \quad \varepsilon_1 = 0 \tag{3.8}$$

and

$$\begin{aligned} g_1(t) &= e^{-a_2 t} - \alpha_0 e^{a_1 t} \\ g_2(t) &= e^{-2a_3 t} - \beta_0 e^{a_1 t} \\ g_3(t) &= e^{a_1 t}. \end{aligned} \tag{3.9}$$

It is readily verified that under the above conditions the exact solution for the system is

$$\begin{aligned} R_1(x,t) &= e^{-(x-a_1 t)} \\ R_2(x,t) &= e^{x-a_2 t} \\ R_3(x,t) &= e^{2(x-a_3 t)}. \end{aligned} \tag{3.10}$$

Thus the analytic solution decays to zero at steady state. The system was discretized by the Lax-Wendroff scheme (2.22) with the following parameters for the numerical boundary conditions (2.26) - (2.27) - (2.28)

$$\begin{aligned} &\alpha_1 = \beta_1 = 0 \\ &\sigma_0 = 1 \quad \varepsilon_0 = 2. \end{aligned} \tag{3.11}$$

Note that at the outflow boundary, $x = 1$, both the analytic and the numerical boundary conditions are in characteristic form, because in this section we are interested in the influence of inflow b.c.'s only.

It can be shown that the inflow determinant condition (3.3) has for the above choice of parameters a solution of the form

$$z_0 = e^{0.3i}. \tag{3.12}$$

The corresponding $\kappa_s(z_0)$ obtained by the quadratic equation (2.30) satisfy

$$|\kappa_1| = .23035 \quad |\kappa_2| = .95334 \quad |\kappa_3| = .19015 \tag{3.13}$$

In the following graphs, we present $w_j^{n,s}$ for several meshes

$$\Delta x = \frac{1}{16}, \frac{1}{32}, \frac{1}{64}, \frac{1}{128} \tag{3.14}$$

Δt was taken to be $0.1\Delta x$, corresponding to a CFL of 0.35 for our flow parameters. The results are sampled at $x = .5, \quad 0 < t \leq 9$; thus

$$j\Delta x = .5 \quad \text{and} \quad 0 < n\Delta t \leq 9. \tag{3.15}$$

At $t = 9$ the analytic solutions $R_s\left(\frac{1}{2}, 9\right)$ $(s = 1, 2, 3)$ are of the order of 10^{-6}.

The numerical solution $w_j^{2,n}$ versus time is presented for $x = .5$ and several meshes in figures: 1(a,b,c,d) for $\frac{1}{\Delta x} = N = 16, 32, 64, 128$. We do not present $w_j^{1,n}$ and $w_j^{3,n}$ because they converge even on coarse meshes $(N \geq 16)$ to the exact solution. This convergent behavior at $x = .5$ is due to the fact that $|\kappa_1|$ and $|\kappa_3|$ are small and hence $|\kappa_1|^{N/2}$ and $|\kappa_3|^{N/2}$ are already of the same order $(\sim 10^{-6})$ as the analytic solution. On the other hand, $w_{N/2}^{2,n}$ displays a time periodic solution on each of the meshes presented. However, as expected, as the mesh is refined the spurious period is halved and the amplitude decreases. The solution converges with the decreasing mesh, but for every one of the fixed meshes used the solution at $x = .5$ still exhibits the spurious frequency, because $|\kappa_2|^{N/2}$ is not yet small enough. This behavior at $x = .5$ is representative of the solution at other spatial locations.

4. The Outflow Case

In this section, we deal with the effects of non-characteristic formulation of the outflow boundary conditions in a similar manner to that of Section 3.

It is easier to do the asymptotic $(N \to \infty)$ analysis in the outflow case by using new coefficients C's. Defining

$$\vec{c} = \begin{pmatrix} C_1 \\ C_2 \\ C_3 \end{pmatrix} \tag{4.1}$$

we may rewrite (2.36) as follows

$$A(\kappa)\vec{a} + D(\mu)\vec{c} = 0 \tag{4.2}$$

$$B(\kappa)\vec{a} + E(\mu)\vec{c} = 0 \tag{4.3}$$

where

$$D(\mu) = A(\mu)\Lambda(\mu) \tag{4.4}$$

$$E(\mu) = B(\mu)\Lambda(\mu) \tag{4.5}$$

with

$$\Lambda(\mu) = \begin{pmatrix} \mu_1^{-N+1} & 0 & 0 \\ 0 & \mu_2^{-N+1} & 0 \\ 0 & 0 & \mu_3^{-N+1} \end{pmatrix} \tag{4.6}$$

and the matrice A and B are defined in (2.35).

Again, for N large, $D(\mu)$ and $E(\mu)$ have small entries. In order to decouple the influence of the inflow conditions, we shall assume $\vec{a} = 0$ and so the determinant condition becomes

$$\det E(\mu) = 0 \tag{4.7}$$

or, more explicitly

$$\det E(\mu) = \mu_1(\mu_2 - 1)(\mu_3 - 1) + \alpha_1\sigma_1\mu_2(\mu_1 - 1)(\mu_3 - 1) + \varepsilon_1\beta_1\mu_3(\mu_1 - 1)(\mu_2 - 1) = 0. \tag{4.8}$$

A technical argument similar to the one leading to (3.4), (3.5) gives a solution of the form

$$w_j^{s,n} = C_s e^{in\omega}\mu_s^{N-j}, \quad \omega \neq 0 \qquad |\mu_s(e^{i\omega n})| > 1 \tag{4.8}$$

The observation made there are also valid here, namely that a spurious solution (as defined there) may exist for non-characteristic outflow treatment; see observations (1) and (2) on pages 7-8. The numerical examples are again based on (2.14) - (2.16) with the same flow parameters, and with the same initial conditions given by (3.7). For the analytic boundary conditions, we took $\alpha_0 = \beta_0 = 0$, $\sigma_1 = 1, \varepsilon_1 = 2$, and, from (2.23) - (2.25),

$$\begin{aligned} g_1 &= e^{-a_2 t} \\ g_2 &= e^{-2a_3 t} \\ g_3 &= e^{a_1 t} + \sigma_1 e^{-a_2 t} + \varepsilon_1 e^{-2a_3 t}. \end{aligned}$$

The analytic solution is again

$$R_1(x,t) = e^{-(x-a_1 t)}, \quad R_2(x,t) = e^{x-a_2 t}, \quad R_3(x,t) = e^{2(x-a_3 t)}. \tag{4.9}$$

The numerical boundary conditions (2.26) - (2.28) imposed on (2.22) were:

$$\alpha_1 = -4.668, \quad \beta_1 = 2.09485, \quad \varepsilon_0 = \sigma_0 = 0. \tag{4.10}$$

These values of α_1 and β_1 were chosen so that we will have a case of a spurious frequency accompanied by at least one μ near to 1. The resulting μ's and z_0 are:

$$|\mu_1| = 1.00625, \quad |\mu_2| = 2.0774, \quad |\mu_3| = 1.3959, \quad z_0 = e^{0.1i}. \tag{4.11}$$

The numerical results for $w_j^{1,n}$ are presented (again at $x = .5$) in Figures 2(a,b,c,d,e). $w_{N/2}^{2,n}$ and $w_{N/2}^{3,n}$ display a convergent behavior due to the smallness of $|\mu_s^{-N+j}|_{j=N/2}, (s = 2,3)$. On the other hand, $w_{N/2}^{1,n}$ is oscillatory on all the meshes we used, although the amplitude decays in accordance with the $\mu_1^{-N/2}$-law.

We have thus demonstrated that spurious frequencies can be induced by improper (i.e., non-characteristic) treatment of boundary conditions, not only at the inflow boundary (see Ref. [1] for the physical case of a flow past a cylinder) but also at the outflow boundary.

5. The Finite Domain Case

In this section, we report on numerical experiments in which both boundaries ($x = 0$ and $x = 1$) are treated in non-characteristic fashion. We chose the same boundary conditions reported on in the previous two sections, but now they are applied simultaneously. Recall that when only the inflow was non-characteristic, the solution exhibited spurious oscillations but the solution converged as $\Delta x \to 0, \Delta t \to 0$. The outflow case on its own exhibited the same behavior. We mention also that the G-K-S theory [2], for the stable case (see Lemma (2.2)), predicts that if the semi-infinite cases (i.e., pure inflow or pure outflow) are each stable separately, then also the finite domain case will be stable and convergent with mesh, though perturbation might grow in time. In the numerical experimentation reported herein, it will be seen that in our special case ($|z_0| = 1$ for each of the semi-infinite problems) the solutions seem to grow exponentially in time and to converge, but non-uniformly, with mesh size.

The numerical approximation (2.22) (for $s = 1,2,3$) was used to solve (2.14) - (2.16) with the boundary conditions now given by:

$$\alpha_0 = 0.582155 \quad \beta_0 = -0.6115 \quad \sigma_0 = 1 \quad \varepsilon_0 = 2 \tag{5.1}$$

$$\alpha_1 = -4.668 \quad \beta_1 = 2.09485 \quad \sigma_1 = 1 \quad \varepsilon_1 = 2 \tag{5.2}$$

The boundary parameters (4.1) were taken from the "pure" inflow problem and those in (4.2) from the "pure" outflow problem.

We show the temporal behavior of $w_j^{1,n}$ at $x = .5$ in Figures 3(a,b,c,d,e,f). Examination of these figures shows that unlike the case of "pure" inflow and outflow, where there were oscillations but they did not grow in time in the present "finite domain" boundary treatment the oscillations grow temporally. $w_j^{2,n}$ and $w_j^{3,n}$ display the same behavior and are not shown here. Another difference between the "pure" case and the present finite-domain case has to do with behavior as Δx is being decreased. In the previous sections, we saw that the amplitude of the oscillation decreased uniformly with the mesh size. In the present case, there is an increase in amplitude as Δx is decreased from $N = 16$ to $N = 128$. Afterwards, for $N = 256$ and 512 we see a decreased amplitude; and although the perturbing oscillations are still large compare to 10^{-6} (and growing temporally) there does seem to be a beginning of convergence.

We should remark here that this type of behavior of the numerical approximation to the solution can be very unsettling for practitioners using practical codes, since multidimensional mesh sizes seem likely not to be in the asymptotic range in the near future.

References

[1] Abarbanel, S., Don, W. S., Gottlieb, D., Rudy, D. H., and Townsend, J. C., *Secondary frequencies in the wake of a circular cylinder with vortex shedding.* ICASE Report No. 90-16 (Feb. 1990). To appear in J. Fluid Mech.

[2] Gustafsson, B., Kreiss, H.-O., and Sundström, A. 1972, "Stability theory of difference approximations for mixed initial boundary value problems II," *Math. Comp.* **26**, 649-686.

[3] Osher, S. 1969, "Systems of differential equations with general homogeneous boundary conditions," *Trans. Amer. Math. Soc.*, **137**, 177-201.

[4] MacCormack, R. W. 1971, in *Lecture Notes in Physics*, Vol. 8, p. 151, Springer-Verlag, New York/Berlin.

[5] Godunov, S. K. and Riabenkii, V. S. 1964, "Introduction to the Theory of Difference Equations," Interscience Published.

[6] Townsend, J. C., Rudy, D. H., and Sirovich, L. 1987, "Computation and analysis of a cylinder wake flow," in *Forum on Unsteady Flow Separation*, (ed., K. N. Ghia) 165-174. ASME.

Figure 1a. $w_{N/2}^{2,n}$ vs. $t \leq 9$ (Inflow, $N = 16$)

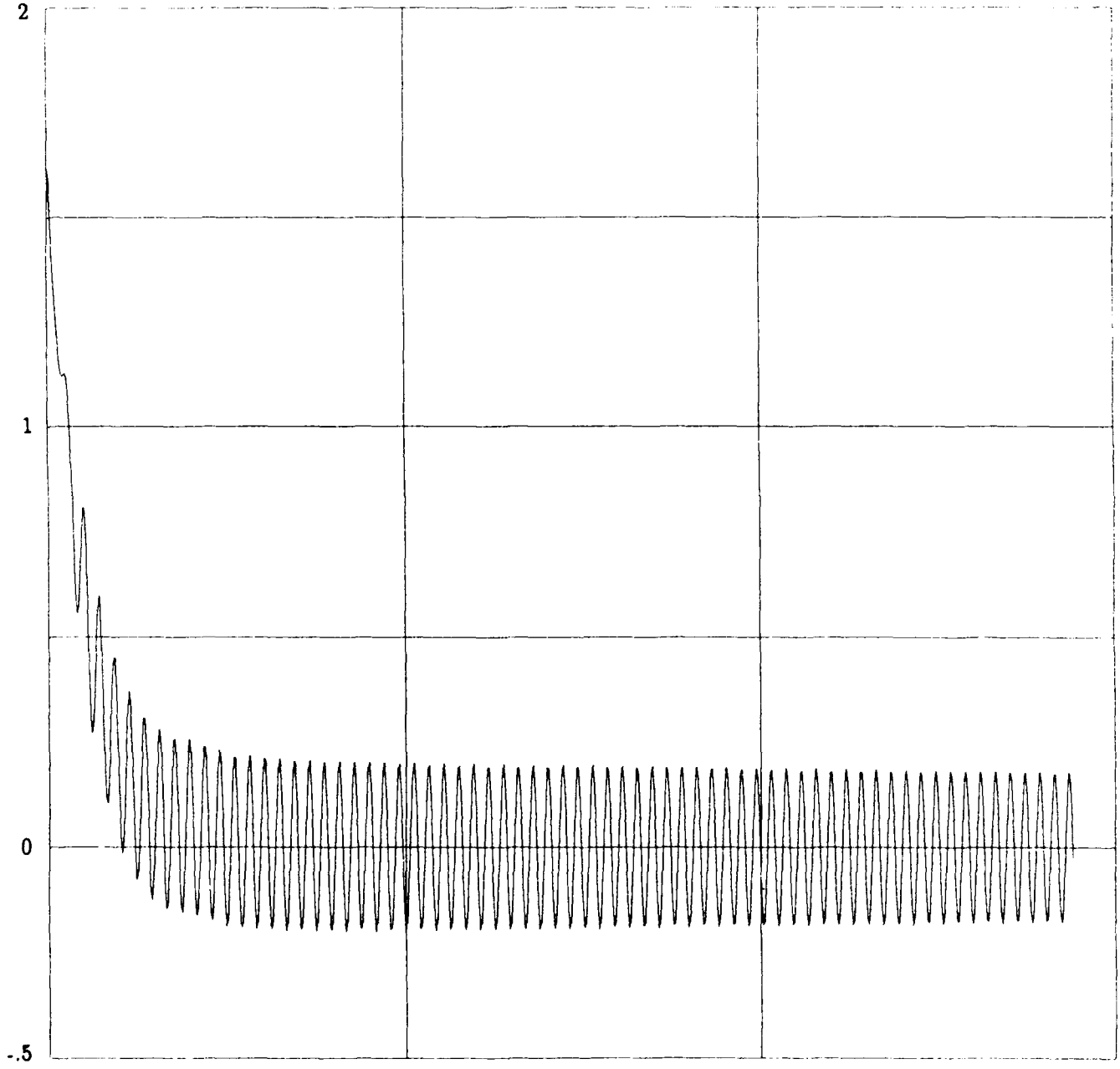

Figure 1b. $w_{N/2}^{2,n}$ vs. $t \leq 9$ (Inflow, $N = 32$)

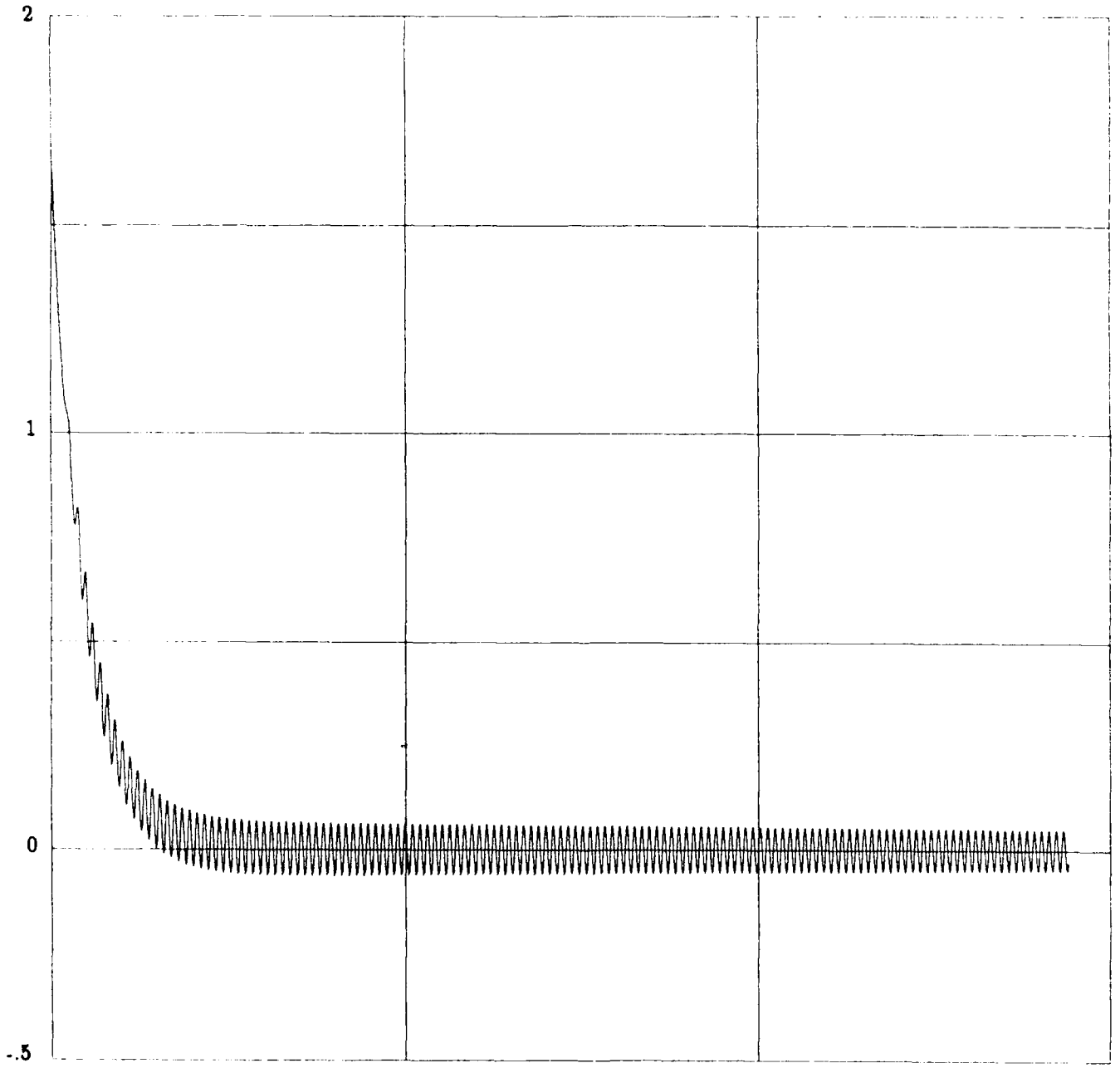

Figure 1c. $w^{2,n}_{N/2}$ **vs.** $t \leq 9$ (Inflow, $N = 64$)

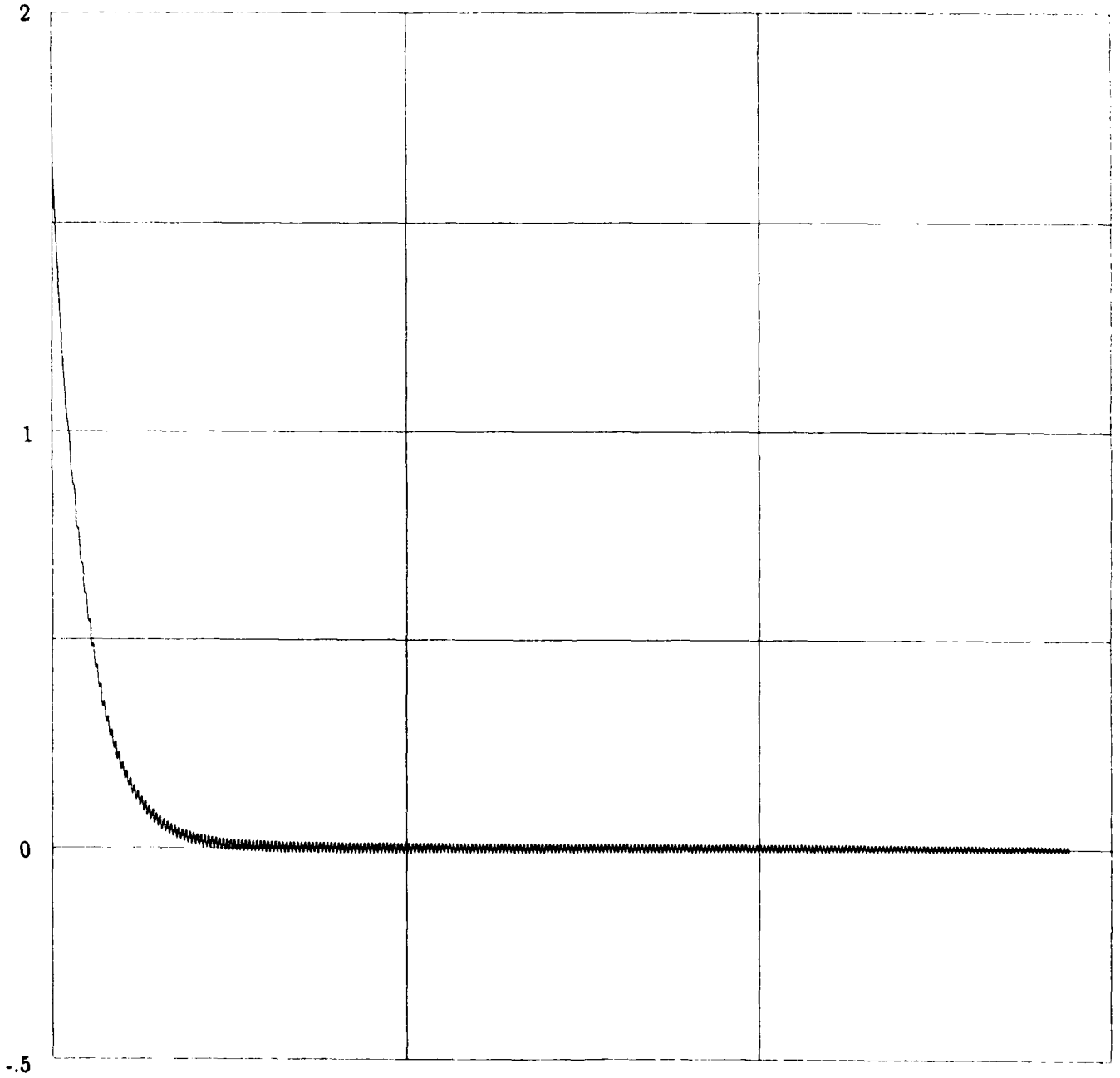

Figure 1d. $w^{2,n}_{N/2}$ vs. $t \leq 9$ (Inflow, $N = 128$)

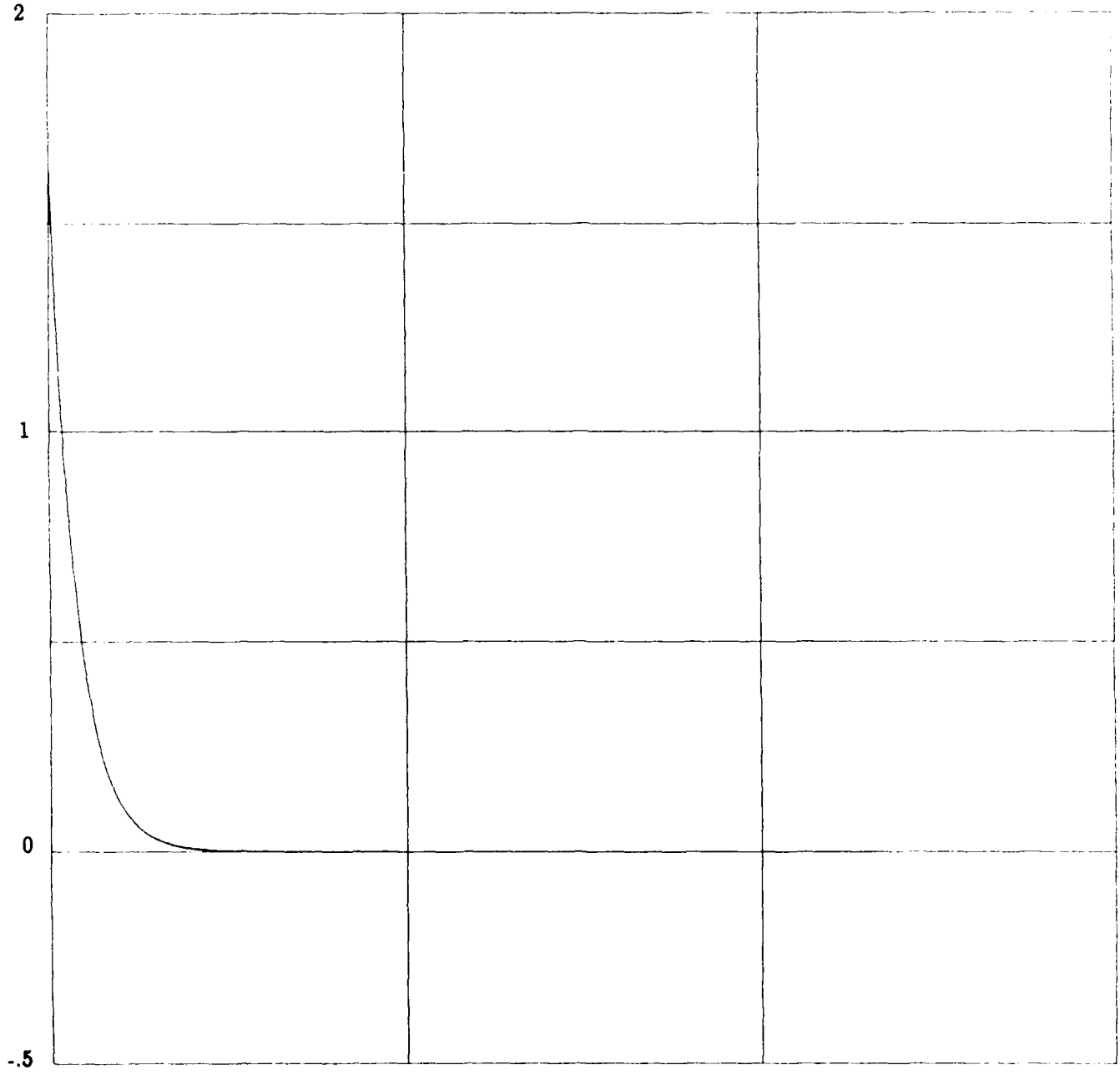

Figure 2a. $w^{1,n}_{N/2}$ vs. $t \leq 9$ (Outflow, $N = 16$)

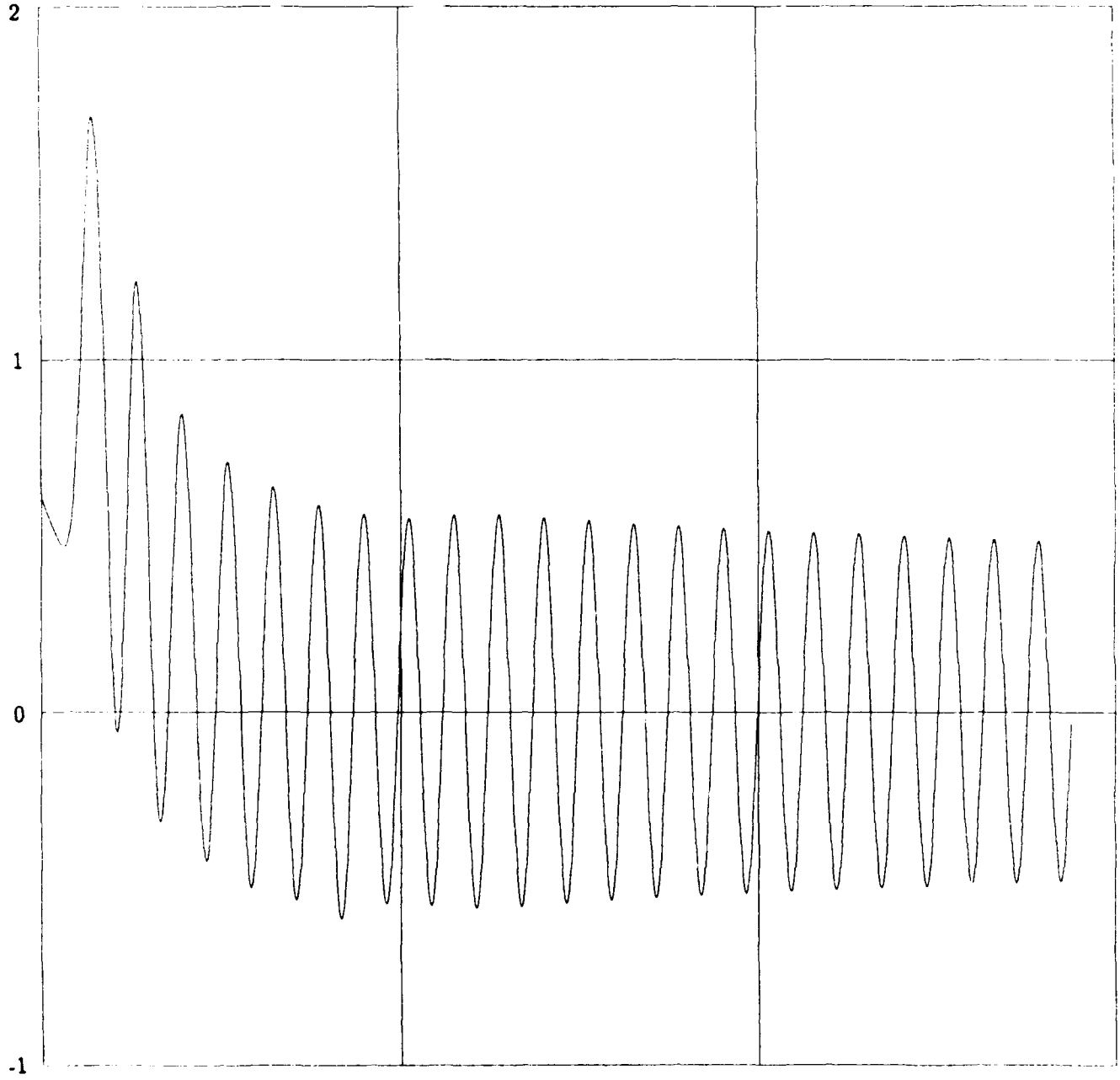

Figure 2b. $w^{1,n}_{N/2}$ vs. $t \leq 9$ (Outflow, $N = 32$)

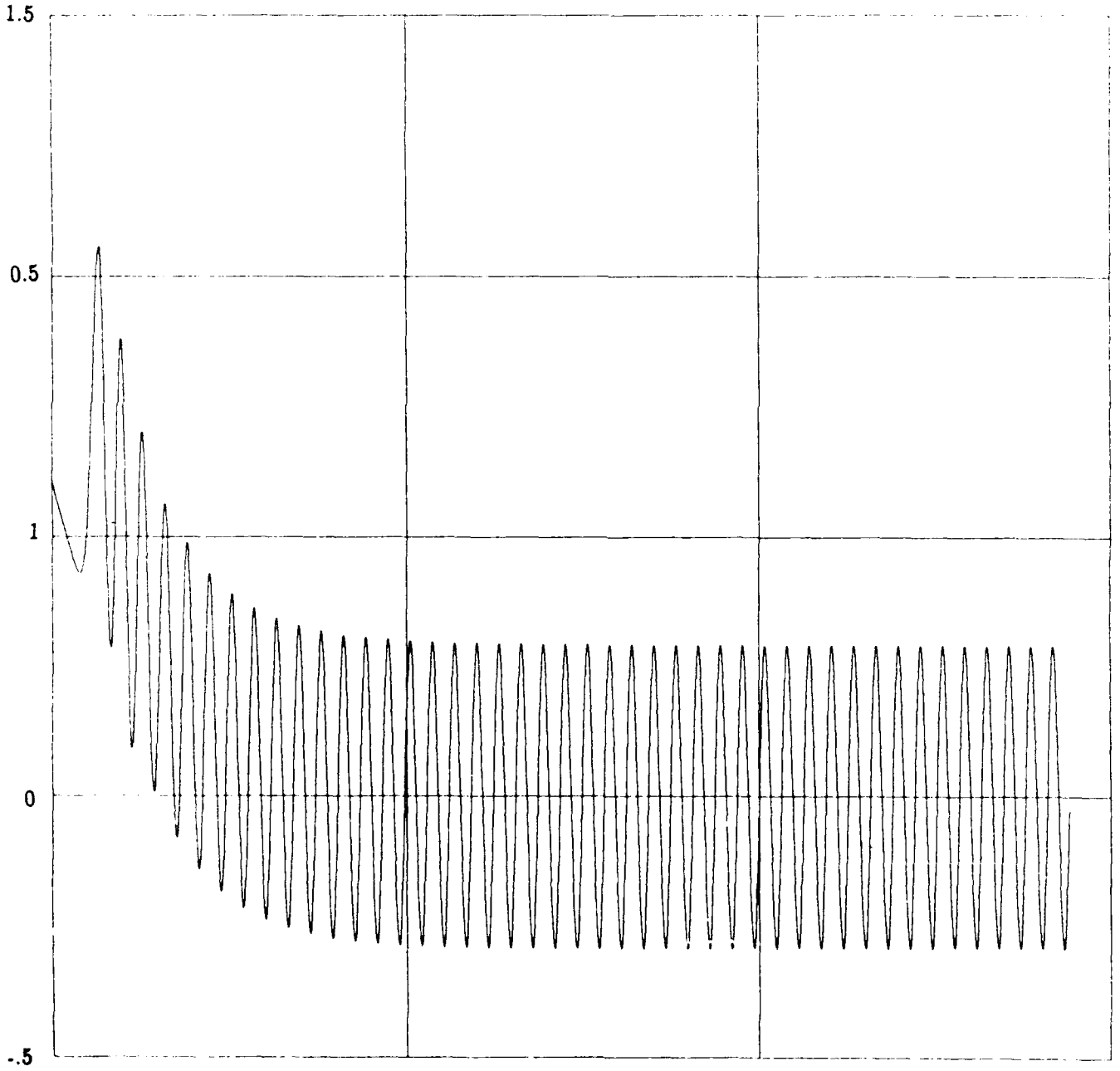

Figure 2c. $w_{N/2}^{1,n}$ vs. $t \leq 9$ (Outflow, $N = 64$)

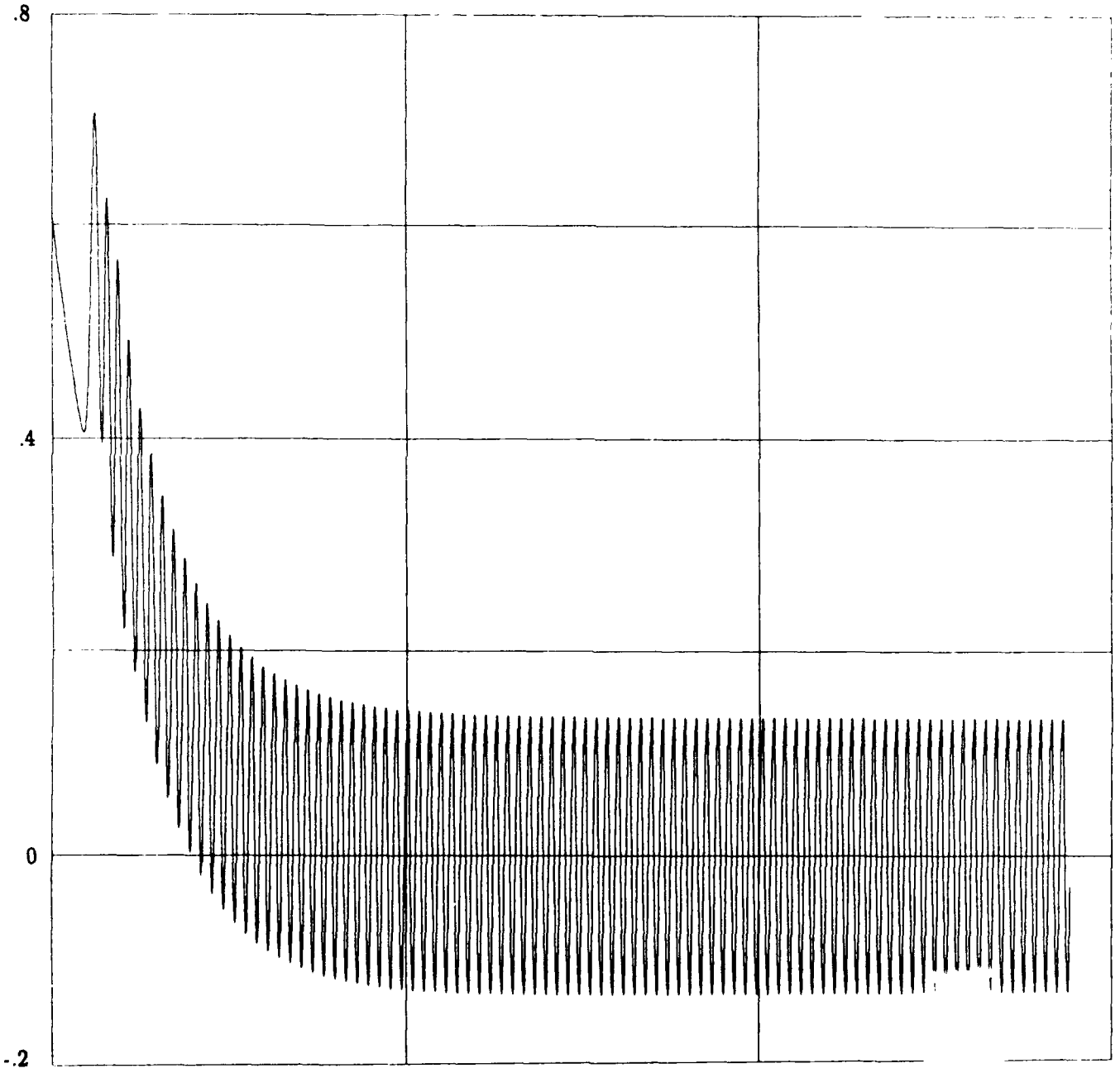

Figure 2d. $w_{N/2}^{1,n}$ vs. $t \leq 9$ (Outflow, $N = 128$)

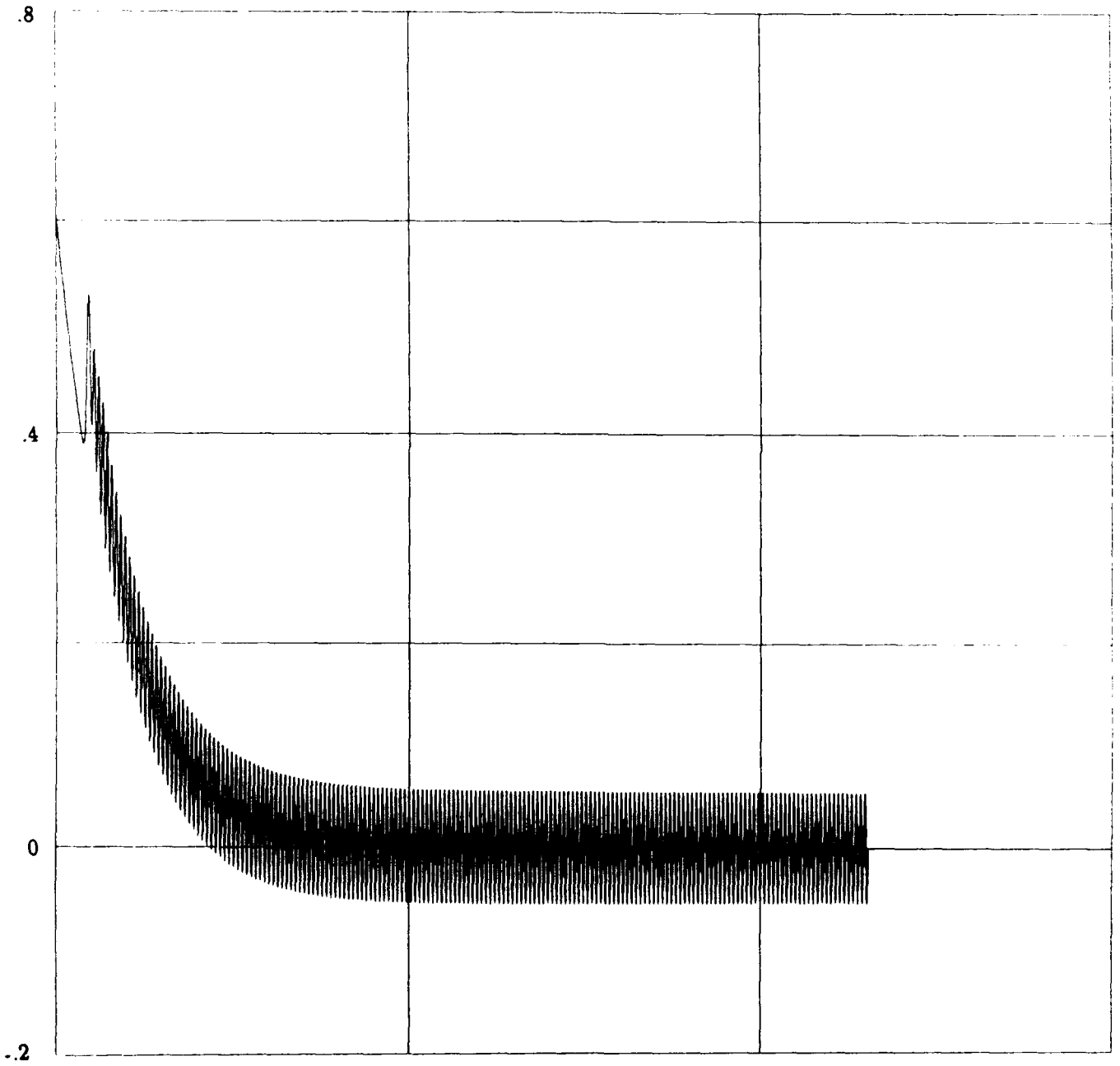

Figure 3a. $w_{N/2}^{1,n}$ vs. $t \leq 9$ (Finite Domain, $N = 16$)

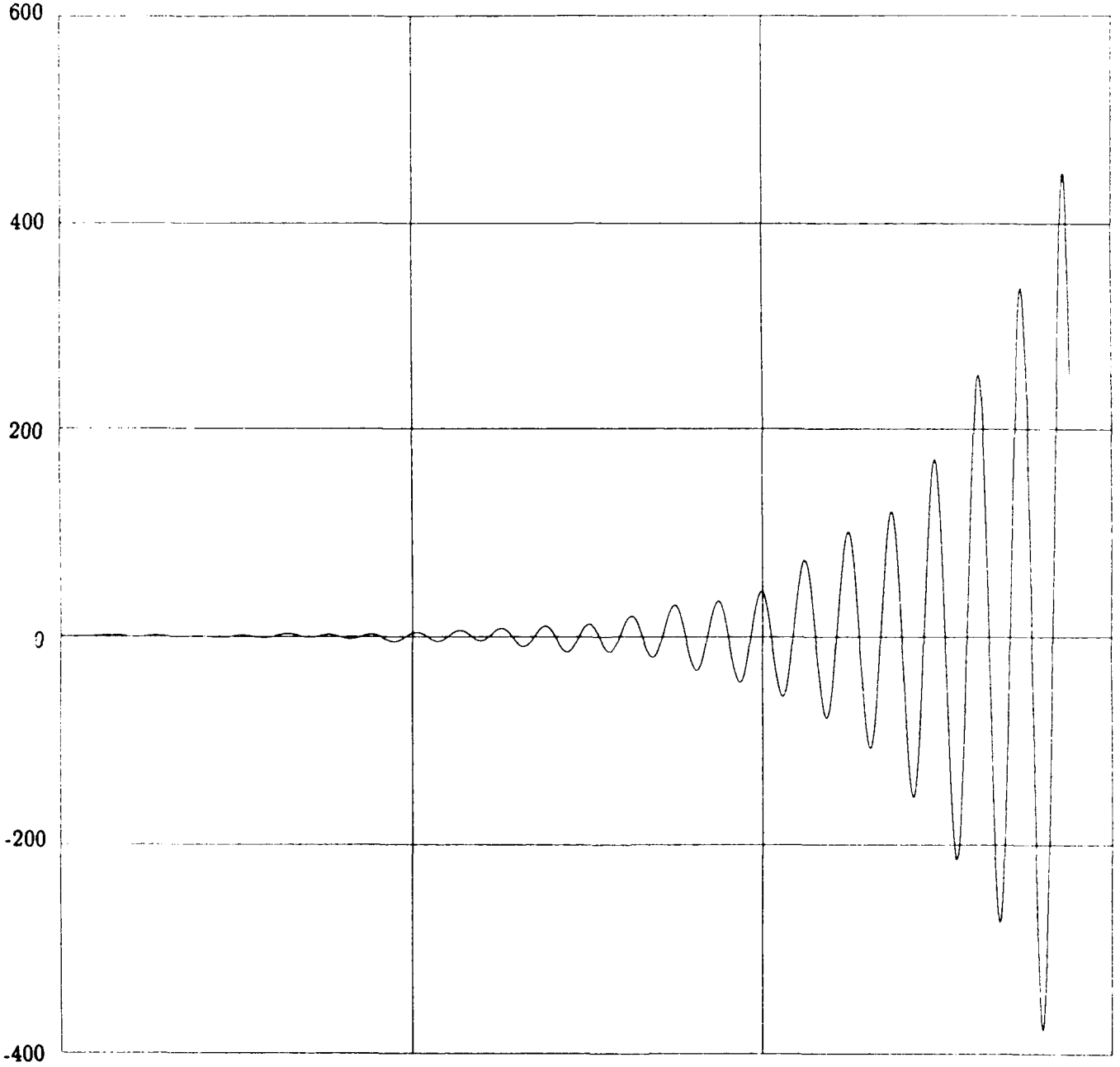

Figure 3b. $w_{N/2}^{1,n}$ vs. $t \leq 9$ (Finite Domain, $N = 32$)

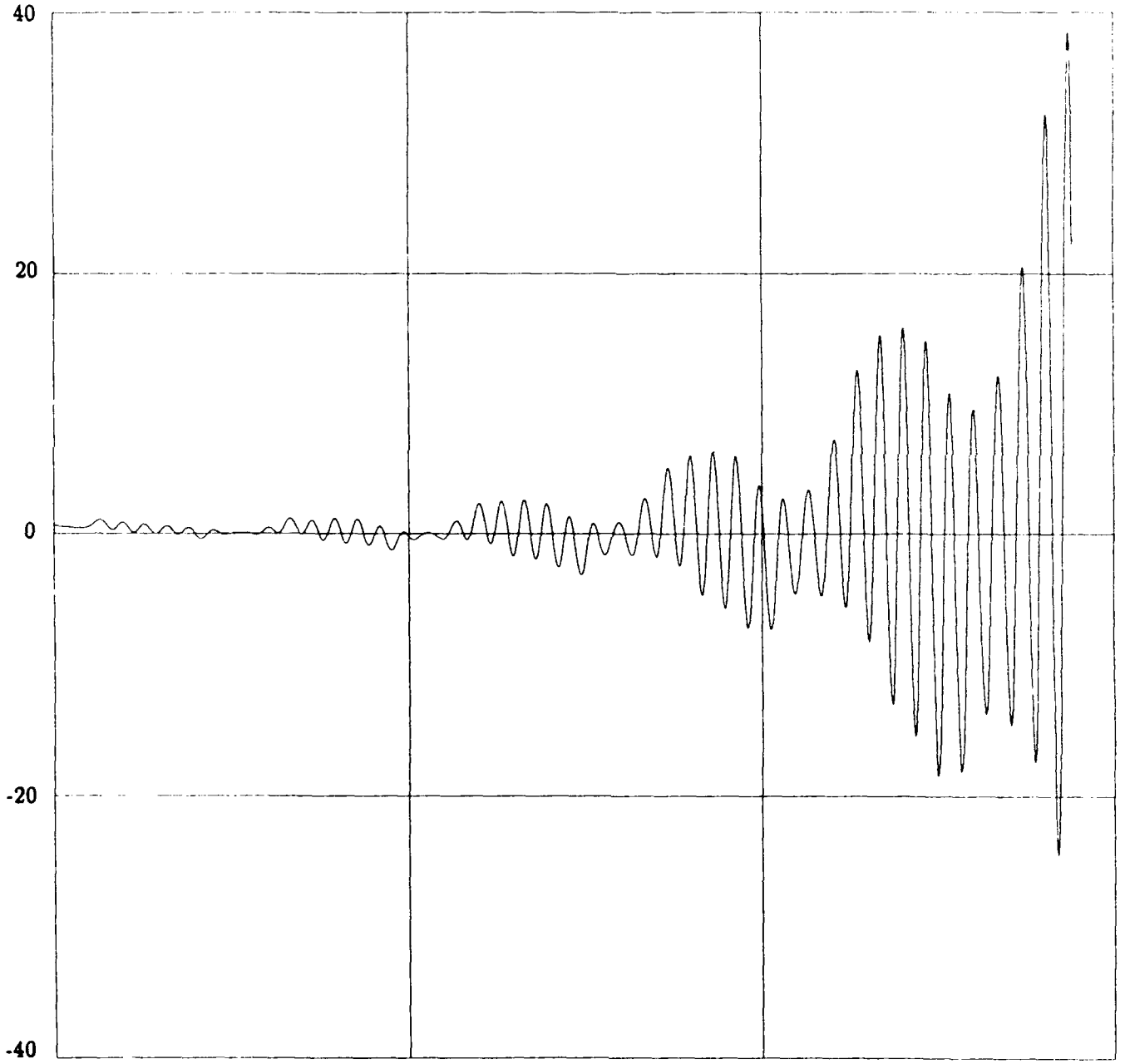

Figure 3c. $w_{N/2}^{1,n}$ vs. $t \leq 9$ (Finite Domain, $N = 64$)

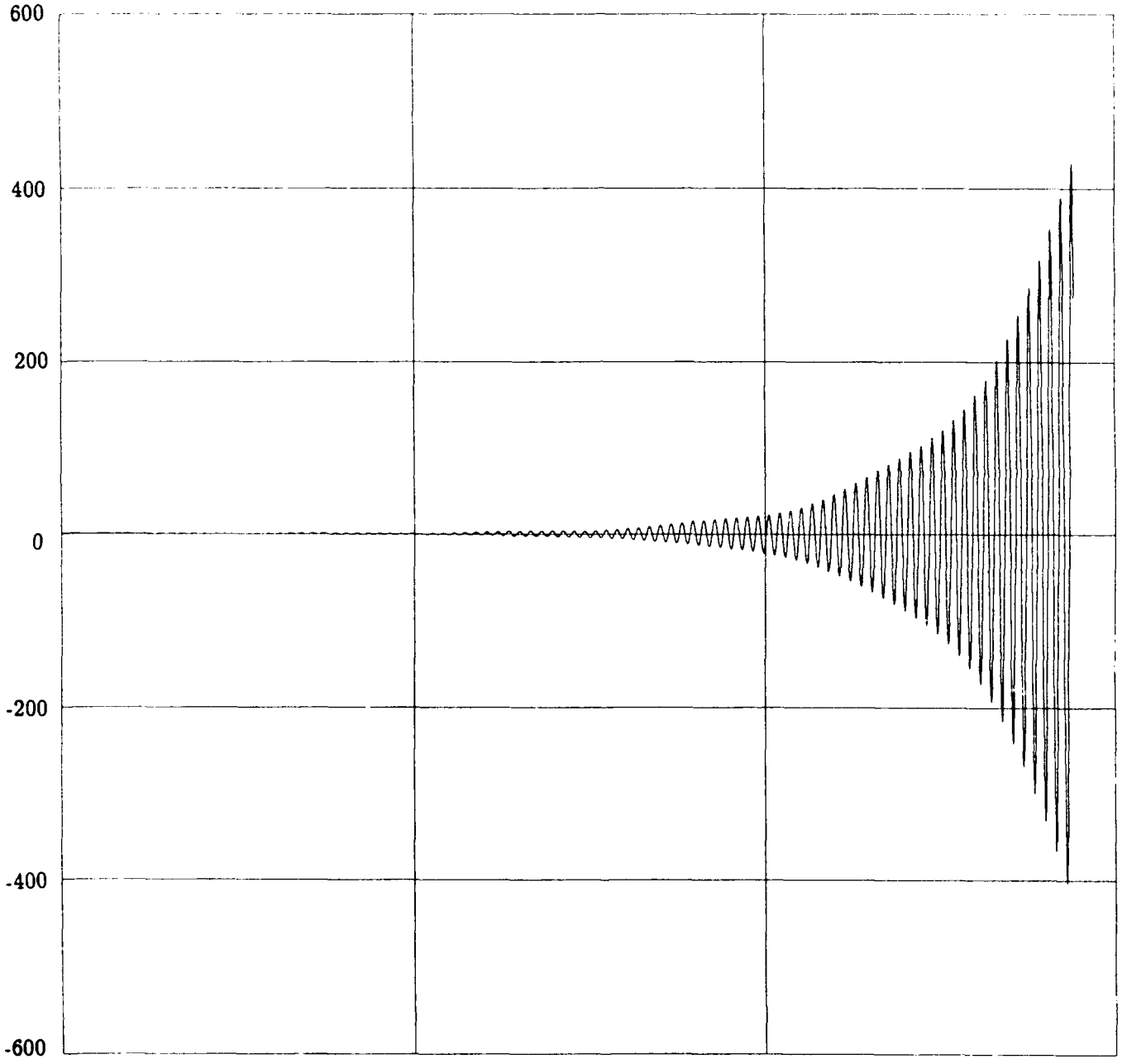

Figure 3d. $w_{N/2}^{1,n}$ vs. $t \leq 9$ (Finite Domain, $N = 128$)

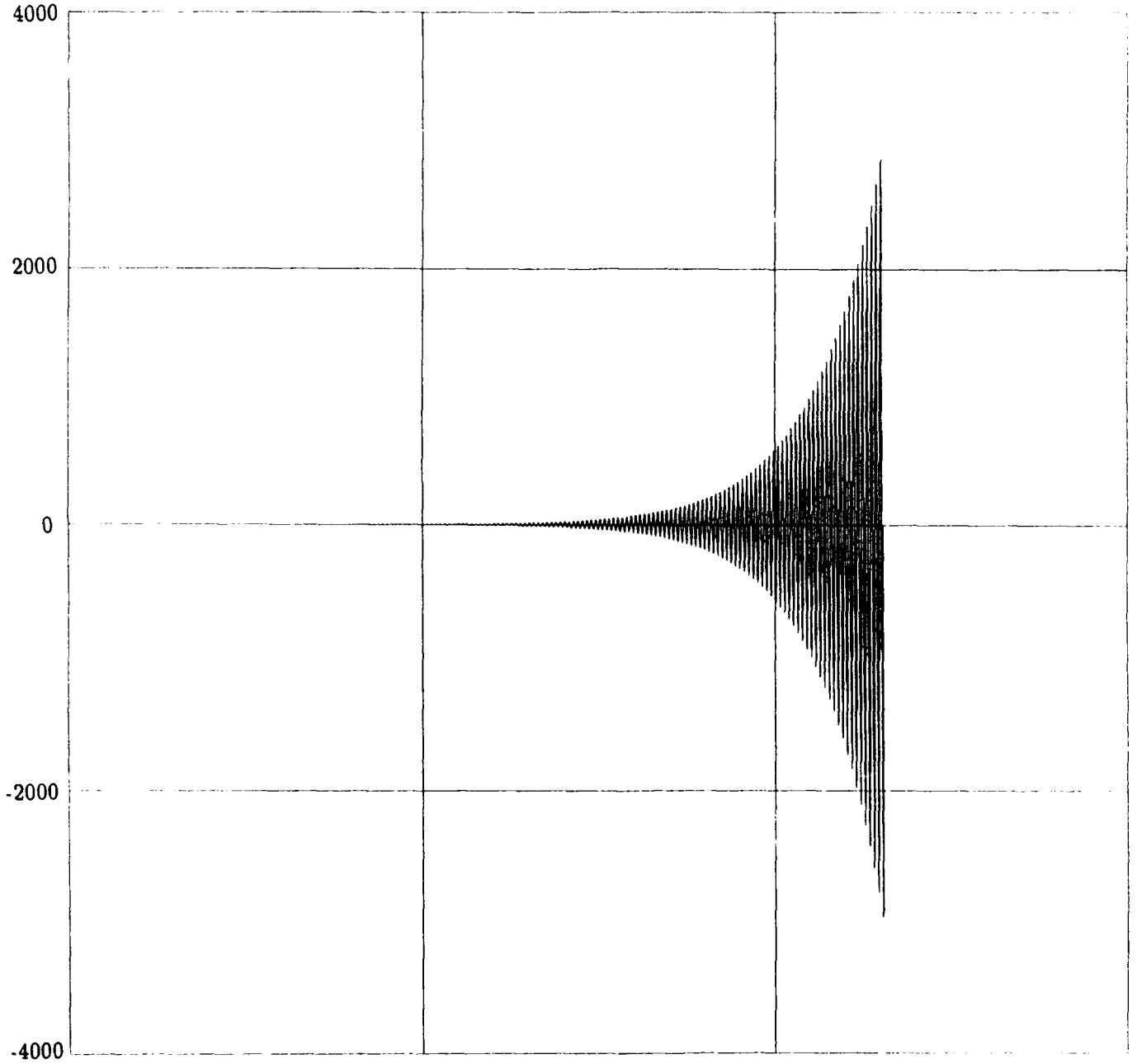

Figure 3e. $w_{N/2}^{1,n}$ vs. $t \leq 9$ (Finite Domain, $N = 256$)

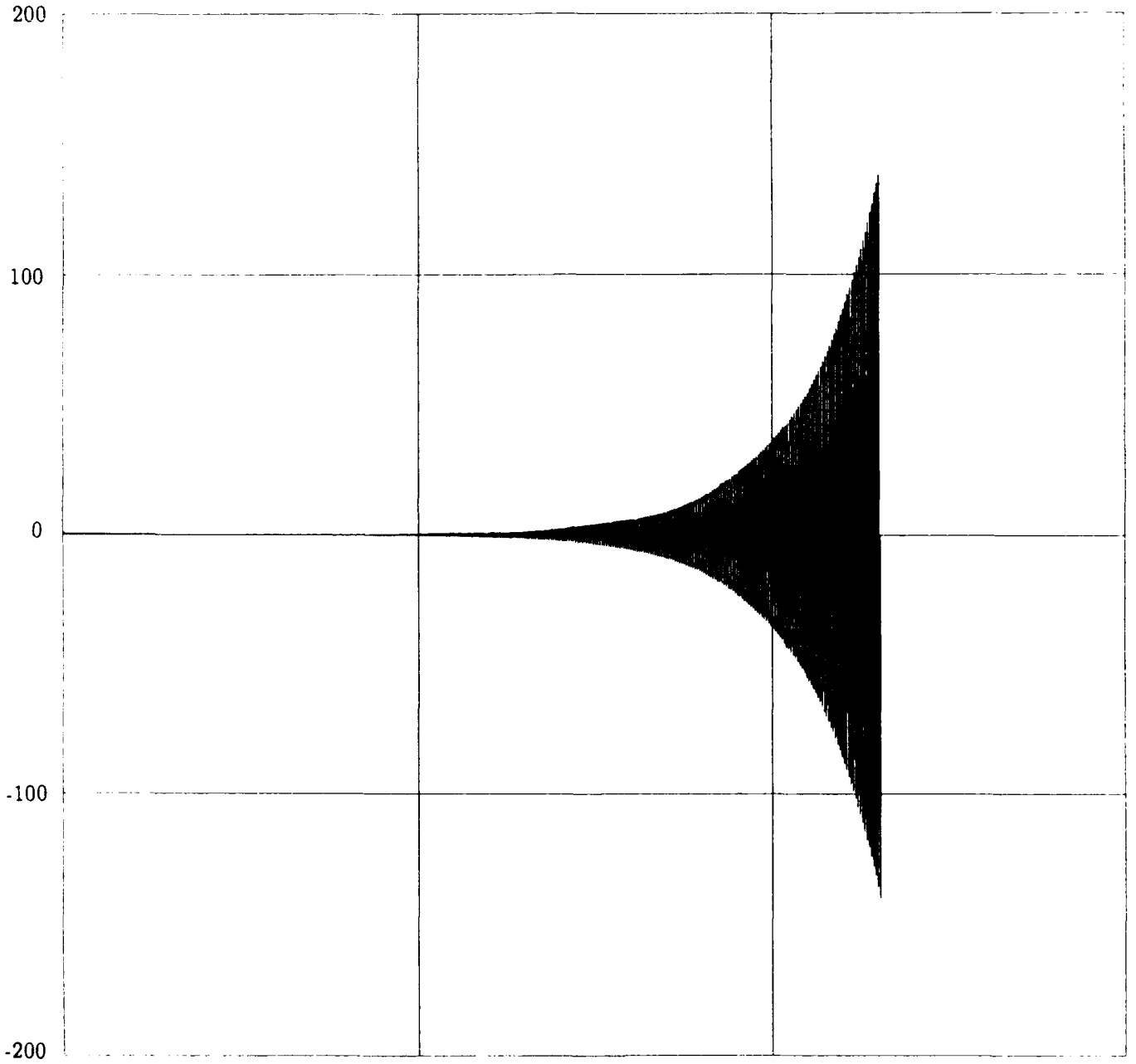

Figure 3f. $w^{1,n}_{N/2}$ vs. $t \leq 9$ (Finite Domain, $N = 512$)

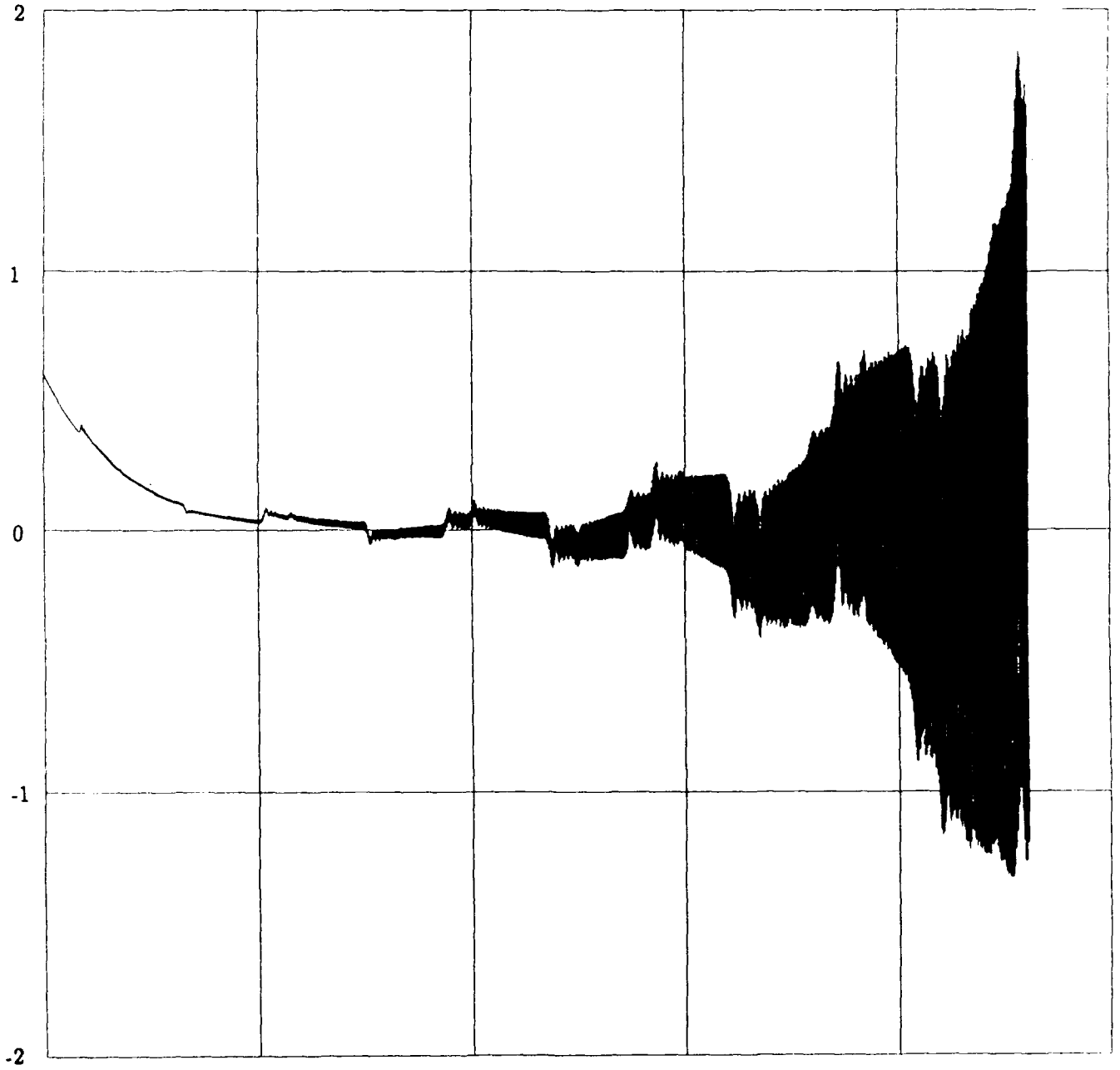

NASA

Report Documentation Page

1. Report No.	2. Government Accession No.	3. Recipient's Catalog No.
NASA CR-187457 ICASE Report No. 90-73		

4. Title and Subtitle	5. Report Date
SPURIOUS FREQUENCIES AS A RESULT OF NUMERICAL BOUNDARY TREATMENTS	October 1990
	6. Performing Organization Code

7. Author(s)	8. Performing Organization Report No.
Saul Abarbanel David Gottlieb	90-73
	10. Work Unit No.
	505-90-21-01
9. Performing Organization Name and Address	11. Contract or Grant No.
Institute for Computer Applications in Science and Engineering Mail Stop 132C, NASA Langley Research Center Hampton, VA 23665-5225	NAS1-18605
	13. Type of Report and Period Covered
12. Sponsoring Agency Name and Address	Contractor Report
National Aeronautics and Space Administration Langley Research Center Hampton, VA 23665-5225	14. Sponsoring Agency Code

15. Supplementary Notes

Langley Technical Monitor:
Richard W. Barnwell

To appear in Proceedings of the Third International Conference on Hyperbolic Systems

Final Report

16. Abstract

The stability theory for finite difference Initial Boundary-Value approximations to systems of hyperbolic partial differential equations states that the exclusion of eigenvalues and generalized eigenvalues is a sufficient condition for stability. The theory, however, does not discuss the nature of numerical approximations in the presence of such eigenvalues.

In fact, as was shown previously (1), for the problem of vortex shedding by a 2-D cylinder in subsonic flow, stating boundary conditions in terms of the primitive (non-characteristic) variables may lead to such eigenvalues, causing perturbations that decay slowly in space and remain periodic time. Characteristic formulation of the boundary conditions avoided this problem.

In this paper, we report on a more systematic study of behavior of the (linearized) one-dimensional gas dynamic equations under various sets of oscillation-inducing "legal" boundary conditions.

17. Key Words (Suggested by Author(s))	18. Distribution Statement
Euler equations; boundary conditions; spurious oscillations	34 - Fluid Mechanics and Heat Transfer 64 - Numerical Analysis Unclassified - Unlimited

19. Security Classif. (of this report)	20. Security Classif. (of this page)	21. No. of pages	22. Price
Unclassified	Unclassified	28	A03

NASA FORM 1626 OCT 86